nature climate change

BRIEF COMMUNICATION

https://doi.org/10.1038/s41558-022-01290-z

Check for updates

Rapid intensification of the emerging southwestern North American megadrought in 2020–2021

A. Park Williams[1,2] ✉, Benjamin I. Cook[2,3] and Jason E. Smerdon[2]

A previous reconstruction back to 800 CE indicated that the 2000–2018 soil moisture deficit in southwestern North America was exceeded during one megadrought in the late-1500s. Here, we show that after exceptional drought severity in 2021, ~19% of which is attributable to anthropogenic climate trends, 2000–2021 was the driest 22-yr period since at least 800. This drought will very likely persist through 2022, matching the duration of the late-1500s megadrought.

Since the year 2000, southwestern North America (SWNA, 30–45° N, 105–125° W) has been unusually dry due to low precipitation totals and heat, punctuated most recently by exceptional drought in 2021[1]. From 2000 to 2021, mean water-year (October–September) SWNA precipitation was 8.3% below the 1950–1999 average and temperature was 0.91 °C above average (Extended Data Fig. 1). No other 22-yr period since at least 1901 was as dry or as hot. While there have been single-year breaks in these anomalous conditions, aridity has dominated the 2000s, as evidenced by declines in two of North America's largest reservoirs, Lakes Mead and Powell, both on the Colorado River. In summer 2021, these reservoirs reached their lowest levels on record, triggering unprecedented restrictions on Colorado River usage[2], in part because the 2-yr naturalized flow out of Colorado River's upper basin in water-years 2020–2021 was likely the lowest since at least 1906 (Extended Data Fig. 2). Aridity was especially extreme and widespread from summer 2020 through summer 2021 (Extended Data Fig. 3). Despite an active North American monsoon in 2021, the United States Drought Monitor (USDM[3]) classified >68% of the western United States as under extreme or exceptional drought for nearly all of July–October 2021 (Extended Data Fig. 4), a record-high proportion of drought extent in the USDM's 22-yr history.

Soil moisture is a particularly important integrator of drought. Soil moisture impacts runoff ratios and therefore streamflow, agricultural productivity and irrigation demand, ecosystem productivity and health, wildfire activity and land–atmosphere feedbacks such as heatwave intensity. Summer soil moisture is particularly crucial, as summer is when water demand from ecosystems, humans and the atmosphere is generally highest, and also the season of focus in most tree-ring reconsructions of drought severity[4]. According to a bucket-type water-balance model forced by monthly climate data[5], SWNA 0–200 cm soil moisture in summer (June–August) was below average in 18 of the 22 years from 2000–2021 (Extended Data Fig. 5). This turn-of-the-twenty-first-century drought was last investigated by Williams et al.[5] through 2018, who speculated that the extended drought event may have been terminating in 2019 due to abundant precipitation that year. Dry conditions returned in 2020 and intensified substantially in 2021, however, indicating that the turn-of-the-twenty-first-century drought is not over.

To understand the longer-term context of the turn-of-the-twenty-first-century drought in SWNA, Williams et al.[5] extended the SWNA summer soil moisture record back to 800 CE using a tree-ring reconstruction and compared the observed drought of 2000–2018 to the infamous megadroughts that occurred repeatedly from 800–1600[6]. These megadroughts were multidecade droughts that exceeded any subsequent event through the 1900s in terms of duration and severity[7]. Williams et al.[5] found that the 19-yr soil moisture anomaly from 2000 to 2018 was probably the second driest in at least 1,200 years, exceeded only by a 19-yr interval during the last of the megadroughts, in the late 1500s. The authors refrained from classifying 2000–2018 as an official megadrought because the reconstructed megadroughts lasted longer than 19 yr.

Here, we update the Williams et al.[5] analysis through 2021 to compare the now 22-yr-long turn-of-the-twenty-first-century drought to the reconstructed megadroughts. Our updated SWNA regionally averaged soil moisture reconstruction is highly skilful (cross-validated $R^2 = 0.74 - 0.85$) and nearly identical to that of Williams et al.[5] (Extended Data Fig. 6). We find that 2000–2021 ranks as the driest 22-yr period since at least 800 CE, with a 22-yr mean soil moisture anomaly of 0.87 s.d. (σ) below the 800–2021 mean (Fig. 1a). The second-driest 22-yr period was 1571–1592, with a reconstructed soil moisture anomaly of $-0.83\,\sigma$, although the reconstruction's 95% uncertainty range overlaps with the 2000–2021 anomaly.

The reconstructed megadroughts and the current event were not exclusively dry across time or space but 2000–2021 was particularly dry in both regards. Of all 22-yr periods since 800 CE, only two (1130–1151 and 1276–1297) contained more years with negative soil moisture anomalies than the 18 observed during 2000–2021 (Extended Data Fig. 7a). Subregionally, 2000–2021 drought rankings were generally less severe relative to past megadroughts but 2000–2021 still ranked among the five driest 22-yr periods locally across 61% of SWNA (Fig. 1b). This represents the largest SWNA area to experience a top- five 22-yr drought-severity ranking in at least 1,200 years (Extended Data Fig. 7b).

Exceptionally dry soil in 2021 was critical for the current drought to escalate and overtake the 1500s megadrought as the period with the highest 22-yr mean severity (Fig. 2a). The 2021 soil moisture anomaly ($-2.58\,\sigma$) was nearly as dry as that of 2002 ($-2.59\,\sigma$), the driest year in the 1901–2021 observational record and notable for its severe impacts on forest ecosystems and wildfire[8,9]. The fact

[1]Department of Geography, University of California, Los Angeles, Los Angeles, CA, USA. [2]Lamont-Doherty Earth Observatory of Columbia University, Palisades, NY, USA. [3]NASA Goddard Institute for Space Studies, New York, NY, USA. ✉e-mail: williams@geog.ucla.edu

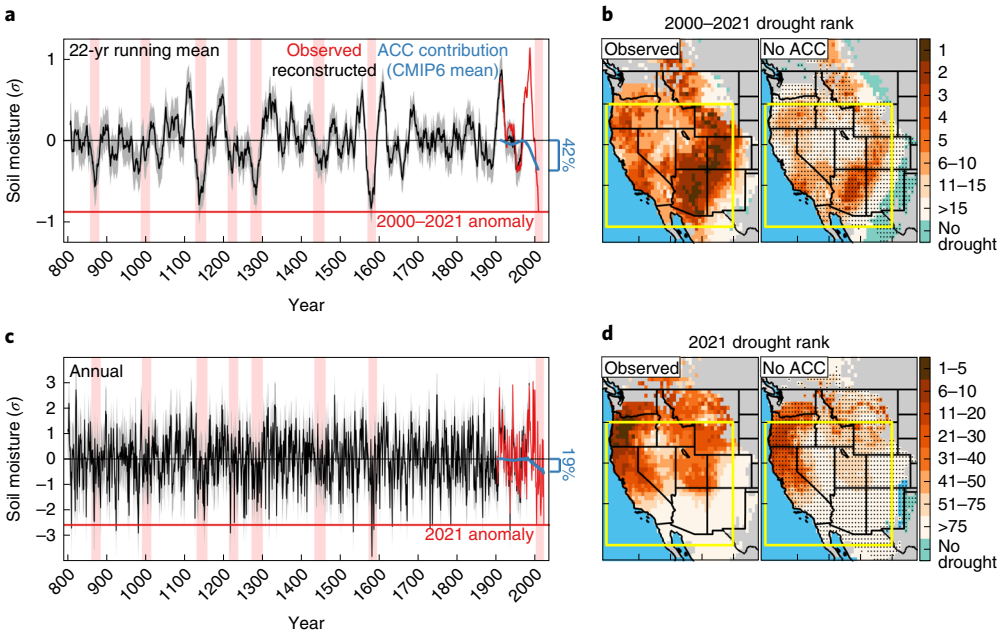

Fig. 1 | Reconstructed and observed soil moisture and the effect of anthropogenic climate trends. a, The 22-yr running mean of June–August 0–200 cm soil moisture anomalies, in units of interannual standard deviations (σ), averaged across SWNA. Reconstructions (black) cover 800–1983 (grey, 95% confidence intervals, CI). Observations (red) and contributions from ACC (blue) cover 1901–2021. Running mean values are displayed in the centre of each 22-yr window. Pink bars, extended drought periods ≥22 yr long. Blue bracket and percentage value to the right indicates the percentage of the observed 2000–2021 soil moisture anomaly accounted for by ACC trends. **b**, Map on the left shows grid-cell specific rankings of 22-yr negative soil moisture anomalies (drought rank) in 2000–2021 compared to the driest 22-yr period in each previous drought event back to 800 CE. The map on the right is the same as the map on the left, but after removal of multimodel mean ACC trends (stippling, 75% of CMIP6 models agree on a net ACC drying effect in 2000–2021; turquoise, above average 2000–2021 soil moisture; grey, excluded due to lack of drought-sensitive tree-ring records back to 800 CE). **c**, Same as **a** but for annual data and the contribution of ACC trends to the 2021 soil moisture anomaly (blue lines represent the same data in both panels **a** and **c** but are 22-yr running means in **a**. **d**, Same as **b** but rankings are for single-year drought severity in 2021 compared to all years back to 800 CE. Geographic boundaries in maps were accessed through Matlab 2020a.

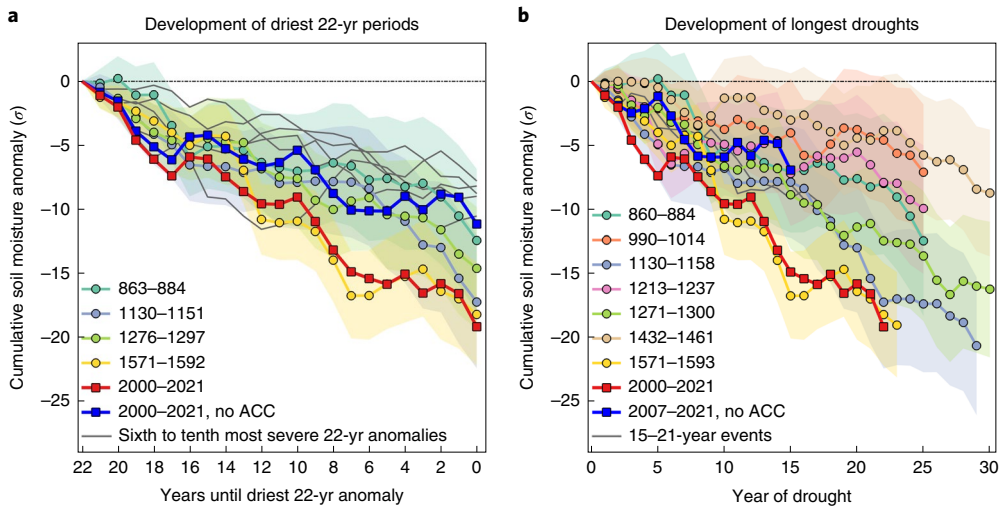

Fig. 2 | Trajectories of the most severe and longest extended droughts since 800 CE. a,**b**, Time series of cumulative SWNA soil moisture anomalies, in σ, during the development of the most negative 22-yr mean soil moisture anomalies (**a**) and from the beginning of all drought events ≥15 yr long (**b**). Blue line, development of the 2000s drought after removing CMIP6 multimodel mean climate trends (no ACC) from the observed trajectory of the 2000s drought (red line). In **b**, each drought period ends in its final year (based on our definition of an extended drought event, described in Methods, the longest megadroughts lasted 30 yr). Note: the blue ACC line is shorter than the red observed line in **b** because the drought would not have started until 2007 in the absence of ACC contributions. Shading, 95% CI for the reconstructed droughts.

that the 2021 drought was comparable to that of 2002 is especially remarkable given high precipitation totals in summer 2021 across much of southern SWNA.

Both 2002 and 2021 were probably drier than any other year in nearly three centuries and they rank as the respective 11th and 12th driest years during the full 800–2021 study period (Fig. 1c). The

most severe reconstructed drought year was 1580 (−3.82 σ) and the most recent year drier than 2002 was 1729 (−2.70 σ). While the 2002 and 2021 drought severities are also exceeded by the reconstructed value for 1934 (−2.80 σ), the observation-based value for that year, which we prioritize, is less severe (−2.12 σ).

We also updated the Williams et al.[5] assessment of the influence of anthropogenic climate change (ACC), now considering climate-model simulations from the Coupled Model Intercomparison Project Phase 6 (CMIP6; ref. [10]). We compare the observation-based record of SWNA soil moisture to that simulated under a counterfactual climate without post-1901 ACC trends in temperature, humidity and precipitation (Extended Data Fig. 8a). The difference between the original and counterfactual soil moisture records is the contribution from ACC trends, displayed as the bold blue time series in Fig. 1a,c. Using the 29 CMIP6 models with adequate data, the multimodel mean ACC trends account for 42% of the SWNA soil moisture anomaly in 2000–2021 and 19% in 2021. The larger contribution of ACC to the 22-yr anomaly arises because background drying from ACC generally influences multidecade mean conditions more than higher-frequency anomalies.

The 42% ACC contribution for 2000–2021 is similar to the 46% value previously found for 2000–2018 using the CMIP5 generation of climate models[5], suggesting little change to how models simulate ACC effects on SWNA hydroclimate. There remains a large range of uncertainty around the multimodel mean result, however, due to uncertainty in how ACC affects SWNA precipitation. Nonetheless, all 29 CMIP6 models indicate a net ACC drying effect on SWNA soil moisture as of 2021 (Extended Data Fig. 8b). Models consistently simulate SWNA drying under ACC because warming without compensatory precipitation increases reduces mountain snowpack reservoirs and increases the atmosphere's evaporative demand[11–14]. Furthermore, anthropogenic warming, which is relatively ubiquitous spatially, has promoted recent drought conditions to be more widespread across SWNA and beyond (Fig. 1b,d). Widespread drought is particularly important to systems sensitive to moisture conditions integrated across large spatial scales (for example, Colorado River users[15]).

The turn-of-the-twenty-first-century drought would not be on a megadrought trajectory in terms of severity or duration without ACC (Fig. 2). Figure 2a extends the Williams et al.[5] analysis to show that throughout the 2000s (red line), drought anomalies have accumulated as fast or faster than the most intense 22-yr drought anomalies in the reconstruction and this would have not occurred in the absence of ACC (blue line). In fact, without ACC, 2000–2021 would not even be classified as a single extended drought event (Fig. 2b). See Methods for our definition of an extended drought event and Extended Data Fig. 9 for time series of the droughts shown in Fig. 2b.

At 22-yr long, the turn-of-the-twenty-first-century drought is highly likely to continue through a 23rd year and match the duration of the shortest of the reconstructed megadroughts (1571–1593; Fig. 2b). We reach this conclusion by conducting simulations in which we repeatedly determine how long the current drought would last if it were immediately followed by each of the 1,183 40-yr sequences in our 800–2021 SWNA soil moisture record (Extended Data Fig. 10). When we superimpose these hypothetical future soil moisture anomalies on the mean ACC effect of the past 5 yr (−0.46 σ), the current drought survives through a 23rd year in 94% of simulations and through a 30th year, the duration of the longest megadroughts in our reconstruction (Fig. 2b), in 75% of simulations. Even assuming no future ACC effect, the current drought lasts 23 and 30 yr in 76% and 33% of the sampled sequences, respectively. In reality, ACC-induced drying in SWNA is likely to intensify[16], making these calculations conservative.

Previous work[17] indicated that continued ACC will increasingly enhance the odds of long, widespread and severe megadroughts returning to SWNA after a hiatus of >400 yr. After the driest 22-yr period in at least 1,200 yr, which included two of the driest 12 individual years in at least 1,200 yr, this worst-case scenario[18] already appears to be coming to pass.

Online content

Any methods, additional references, Nature Research reporting summaries, source data, extended data, supplementary information, acknowledgements, peer review information; details of author contributions and competing interests; and statements of data and code availability are available at https://doi.org/10.1038/s41558-022-01290-z.

Received: 10 September 2021; Accepted: 19 January 2022;
Published online: 14 February 2022

References

1. Mankin, J. S. et al. *NOAA Drought Task Force Report on the 2020–2021 Southwestern U.S. Drought* (NOAA Drought Task Force, MAPP and NIDIS, 2021); https://www.drought.gov/sites/default/files/2021-09/NOAA-Drought-Task-Force-IV-Southwest-Drought-Report-9-23-21.pdf
2. *H.R.2030—Colorado River Drought Contingency Plan Authorization Act* (US House of Representatives, 2019); https://www.congress.gov/bill/116th-congress/house-bill/2030
3. Svoboda, M. et al. The Drought Monitor. *Bull. Am. Meteorol. Soc.* **83**, 1181–1190 (2002).
4. Cook, E. R. et al. Megadroughts in North America: placing IPCC projections of hydroclimatic change in a long-term palaeoclimate context. *J. Quat. Sci.* **25**, 48–61 (2010).
5. Williams, A. P. et al. Large contribution from anthropogenic warming to a developing North American megadrought. *Science* **368**, 314–318 (2020).
6. Cook, B. I. et al. North American megadroughts in the Common Era: reconstructions and simulations. *WIREs Clim. Change* **7**, 411–432 (2016).
7. Woodhouse, C. A. & Overpeck, J. T. 2000 years of drought variability in the central United States. *Bull. Am. Meteorol. Soc.* **79**, 2693–2714 (1998).
8. Breshears, D. D. et al. Regional vegetation die-off in response to global-change-type drought. *Proc. Natl Acad. Sci. USA* **102**, 15144–15148 (2005).
9. Williams, A. P. et al. Temperature as a potent driver of regional forest drought stress and tree mortality. *Nat. Clim. Change* **3**, 292–297 (2013).
10. Eyring, V. et al. Overview of the Coupled Model Intercomparison Project Phase 6 (CMIP6) experimental design and organization. *Geosci. Model Dev.* **9**, 1937–1958 (2016).
11. Barnett, T. P., Adam, J. C. & Lettenmaier, D. P. Potential impacts of a warming climate on water availability in snow-dominated regions. *Nature* **438**, 303–309 (2005).
12. Das, T., Pierce, D. W., Cayan, D. R., Vano, J. A. & Lettenmaier, D. P. The importance of warm season warming to western US streamflow changes. *Geophys. Res. Lett.* **38**, L23403 (2011).
13. Milly, P. C. D. & Dunne, K. A. Colorado River flow dwindles as warming-driven loss of reflective snow energizes evaporation. *Science* **367**, 1252–1255 (2020).
14. Pascolini-Campbell, M., Reager, J. T., Chandanpurkar, H. A. & Rodell, M. A 10 per cent increase in global land evapotranspiration from 2003 to 2019. *Nature* **593**, 543–547 (2021).
15. Udall, B. & Overpeck, J. The twenty-first century Colorado River hot drought and implications for the future. *Water Resour. Res.* **53**, 2404–2418 (2017).
16. Cook, B. I. et al. Uncertainties, limits, and benefits of climate change mitigation for soil moisture drought in southwestern North America. *Earth's Future* **9**, e2021EF002014 (2021).
17. Ault, T. R., Mankin, J. S., Cook, B. I. & Smerdon, J. E. Relative impacts of mitigation, temperature, and precipitation on 21st-century megadrought risk in the American Southwest. *Sci. Adv.* **2**, e1600873 (2016).
18. Woodhouse, C. A., Meko, D. M., MacDonald, G. M. & Stahle, D. W. A 1,200-year perspective of 21st century drought in southwestern North America. *Proc. Natl Acad. Sci. USA* **107**, 21283–21288 (2010).

Methods

This study extends the Williams et al.[5] analysis, which ended in 2018, through 2021. Methods are described in detail in that paper. The Supplementary Text describes the updated 0.25° resolution monthly climate dataset we use to force a bucket model to estimate 0.25° monthly 0–200 cm soil moisture plus snow-water equivalent (referred to as soil moisture) for 1901–2021.

Mean June–August soil moisture values are aggregated to 0.5° resolution for tree-ring reconstruction following Williams et al.[5] with minor updates including use of new Sierra Nevada tree-ring records[19]. Each grid cell's final reconstruction comprises the best-performing reconstruction among an ensemble produced using various combinations of calibration period, search radius (maximum distance between a grid cell and a tree-ring site) and spatial smoothing of the reconstruction's target soil moisture dataset (for large search radii, spatial resolution of the target was reduced). Williams et al.[5] allowed for spatial smoothing up to 7.5°. Here, we limit maximum smoothing to 5.5°. In assembling the final reconstruction, we assess ensemble-member performance with the cross-validated Akaike information criterion (Williams et al.[5] used Pearson's correlation) following a recent reconstruction effort[20], which penalizes against additional predictors and rewards longer calibration periods. Gridded reconstructions, the SWNA regionally averaged reconstruction and observation-based time series are restandardized relative to 800–2021 (prioritizing observation-based data during overlap).

To assess climate change impacts we use monthly outputs of precipitation, mean daily maximum and minimum temperature and mean relative humidity simulated by 29 climate models through the CMIP6 historical (1850–2014) and Shared Socioeconomic Pathway SSP2.45 (2015–2100) experiments (Supplementary Table 1). Multimodel mean trends since 1901, assessed as 50-yr filtered time series for temperature and relative humidity and 100-yr filtered time series for precipitation, are considered to represent ACC trends following Williams et al.[5]. Counterfactual records of observed 1901–2021 climate in the absence of ACC trends are calculated by removing ACC trends. The counterfactual climate records were then used to force the bucket model to simulate counterfactual soil moisture.

We define an 'extended drought event' as follows: a record of 10-yr running mean SWNA soil moisture anomaly is calculated, with running means assigned to the final year of each period. Strings of ≥10 consecutive years with negative 10-yr mean values are identified initially as extended events, including all 10 yr that contributed to the first negative running mean value. Events are trimmed at each end to ensure that they begin and end when soil moisture anomalies turn negative and positive, respectively. First, if there were two or more consecutive positive anomalies in the first or last 10 years of an event, these years and the years preceding or following, respectively, were dismissed. Events were further trimmed to not allow the first or last soil moisture anomaly of the event to be positive. Finally, we dismissed any events lasting <5 yr and also considered any string of ≥5 consecutive negative-anomaly years to be an extended drought event.

Data availability

The datasets used by and produced for this study are available at at https://doi.org/10.25921/8pt9-hz08.

Code availability

The code for the analysis in this paper is available on request to the corresponding author.

References

19. Lepley, K. et al. A multi-century Sierra Nevada snowpack reconstruction modeled using upper-elevation coniferous tree rings (California, USA). *Holocene* **30**, 1266–1278 (2020).
20. Williams, A. P. et al. Tree rings and observations suggest no stable cycles in Sierra Nevada cool-season precipitation. *Water Resour. Res.* **57**, e2020WR028599 (2021).

Acknowledgements

We acknowledge funding from NSF AGS-1703029 (A.P.W.), AGS-1805490 (J.E.S.) and AGS-2101214 (J.E.S.); NOAA MAPP NA19OAR4310278 (A.P.W. and B.I.C.) and NA20OAR4310425 (J.E.S.); and DOE DESC0022302 (A.P.W., B.I.C. and J.E.S.). This work is possible due to many contributors of tree-ring data, largely through the International Tree-Ring Databank. Thanks also to J. Littell, who shared raw ring-width measurements that he produced from 18 sites in Idaho, Oregon and Washington.

Author contributions

A.P.W., B.I.C. and J.E.S. conceived of the study. A.P.W. performed the primary analysis and wrote the paper. All authors helped revise the original draft manuscript.

Competing interests

The authors declare no competing interests.

Additional information

Extended data is available for this paper at https://doi.org/10.1038/s41558-022-01290-z.

Supplementary information The online version contains supplementary material available at https://doi.org/10.1038/s41558-022-01290-z.

Correspondence and requests for materials should be addressed to A. Park Williams.

Peer review information *Nature Climate Change* thanks Isla Simpson, Brad Udall and the other, anonymous, reviewer(s) for their contribution to the peer review of this work.

Reprints and permissions information is available at www.nature.com/reprints.

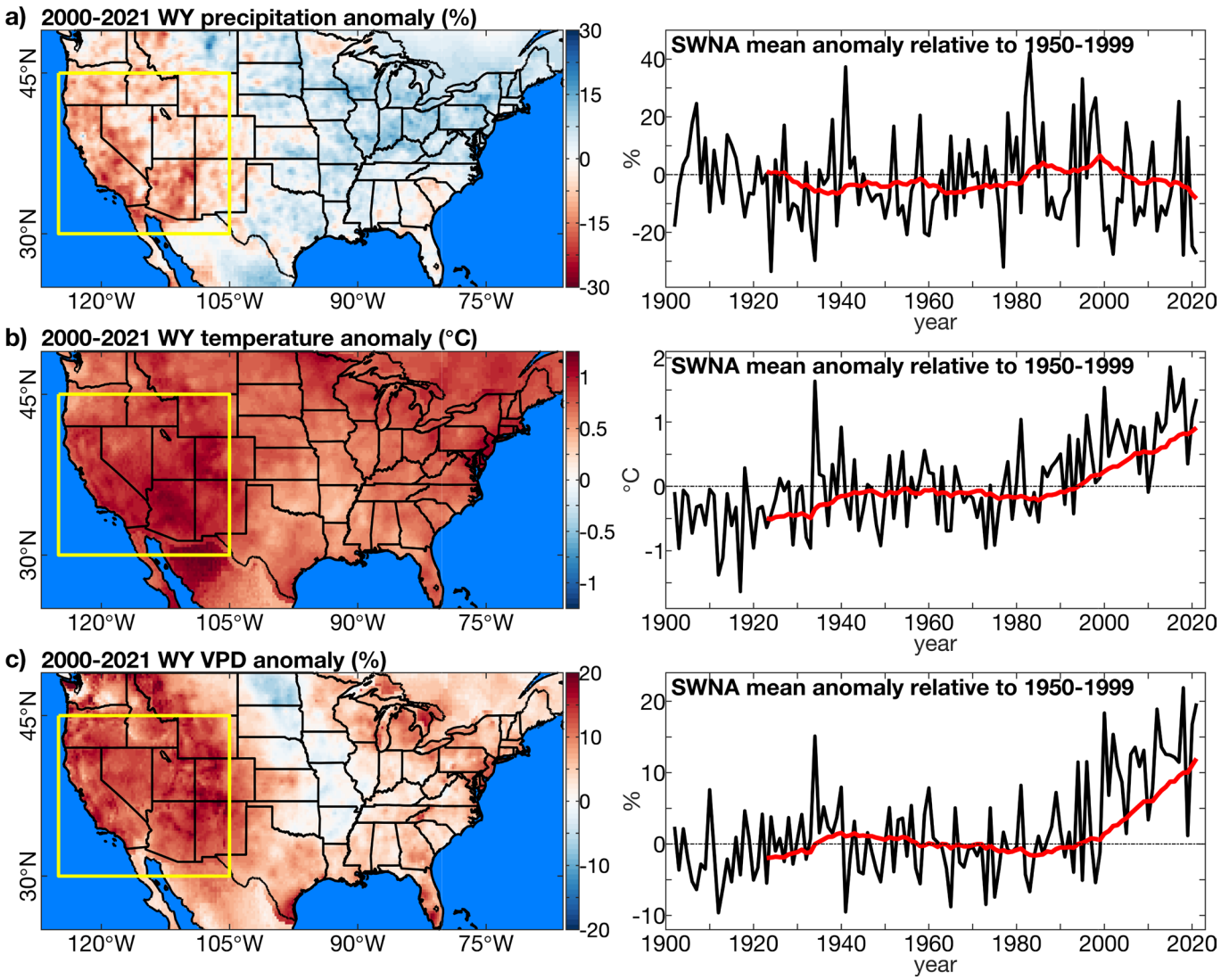

Extended Data Fig. 1 | Observed climate anomalies. Anomalies in water-year (WY: October–September) (**a**) precipitation total, (**b**) temperature, and (**c**) vapour-pressure deficit (VPD). Maps on left show the average WY anomaly during 2000–2021. Yellow box: Southwestern North America (SWNA) study region. Anomalies are relative to 1950–1999. Time series on right show regionally averaged WY anomalies in SWNA (black) annually and as (red) 22-year running means visualized on the final year in each 22-year period. Geographic boundaries in maps were accessed through Matlab 2020a.

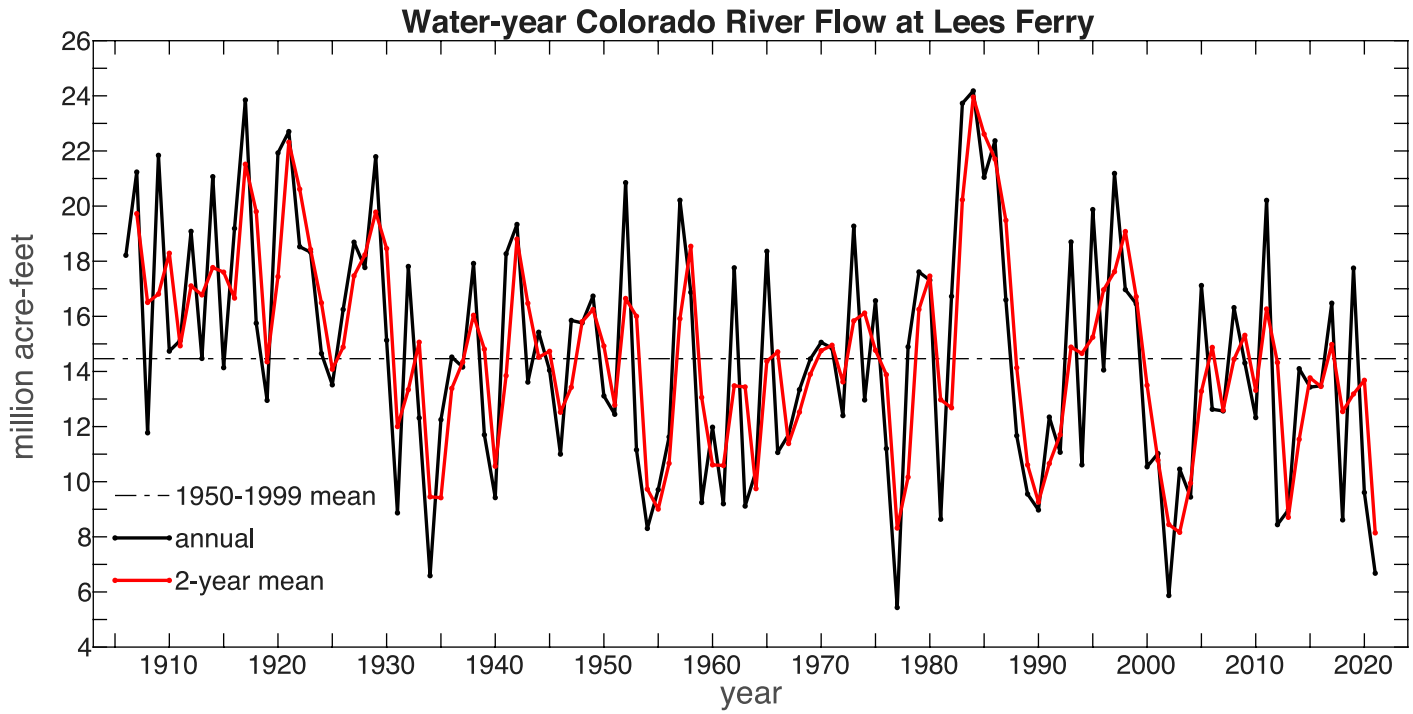

Extended Data Fig. 2 | River flow from the upper basin of the Colorado River. Water-year naturalized flow of the Colorado River at Lees Ferry. Data come from https://www.usbr.gov/lc/region/g4000/NaturalFlow/provisional.html as of January 27, 2022.

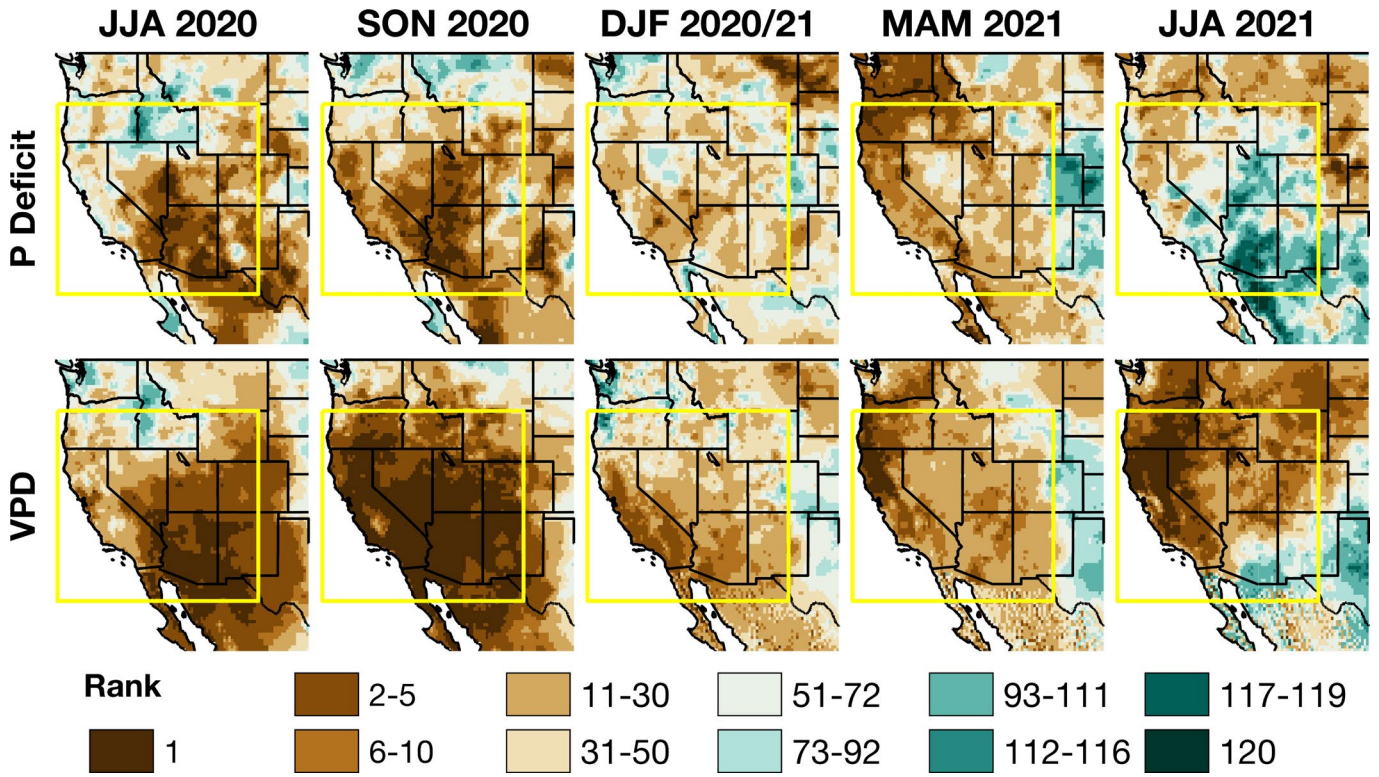

Extended Data Fig. 3 | Seasonal climate in 2020–2021. Seasonal rankings of precipitation (P) deficit (negative precipitation total) and vapour-pressure deficit (VPD) during June–August (JJA) 2020, September–November (SON) 2020, December–February (DJF) 2020–2021, March–May 2021, and June–August (JJA) 2021. Rankings are calculated over the 120-year period from 1902–2021. Geographic boundaries in maps were accessed through Matlab 2020a.

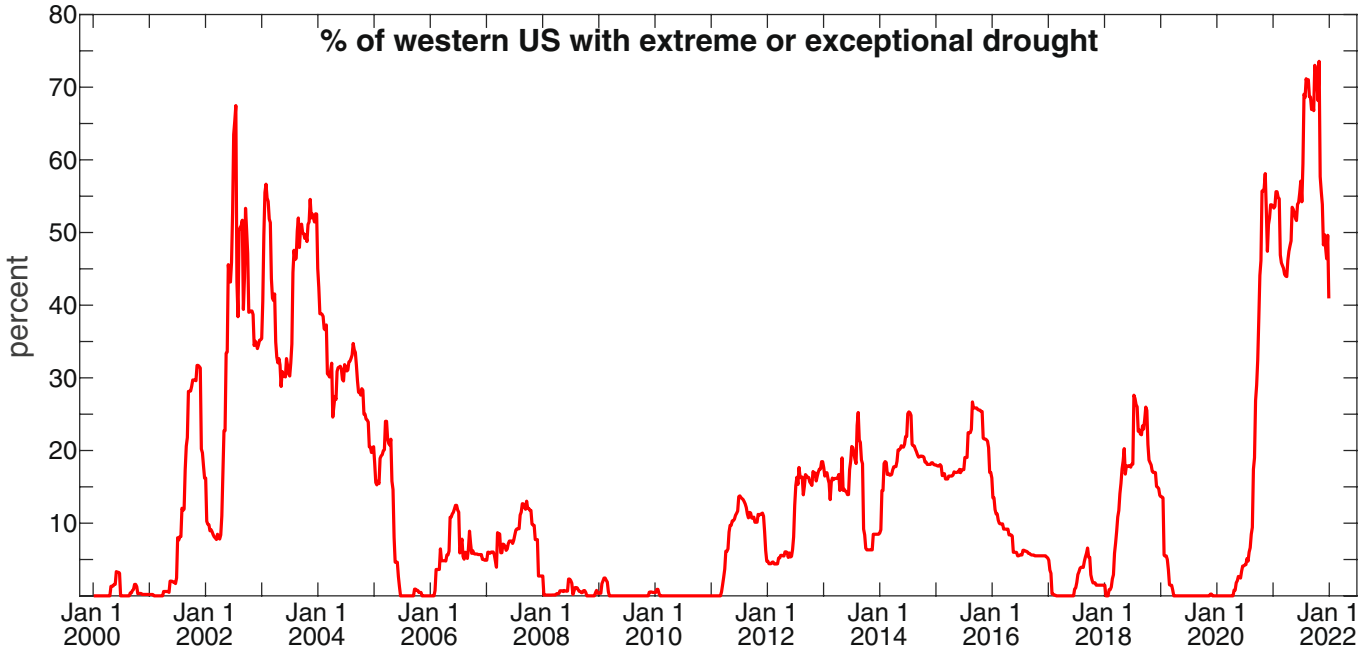

Extended Data Fig. 4 | Extreme and exceptional drought in the western United States (US). Weekly percentage of western continental United States (west of 103°W) classified by the United States Drought Monitor (USDM) as under extreme or exceptional drought from January 1, 2000 to December 28, 2021. Calculations were made form weekly shapefiles of USDM drought classifications, available at https://droughtmonitor.unl.edu/DmData/GISData.aspx as of January 9, 2022. The USDM is developed by the National Drought Mitigation Center (NDMC), the U.S. Department of Agriculture (USDA) and the National Oceanic and Atmospheric Administration (NOAA).

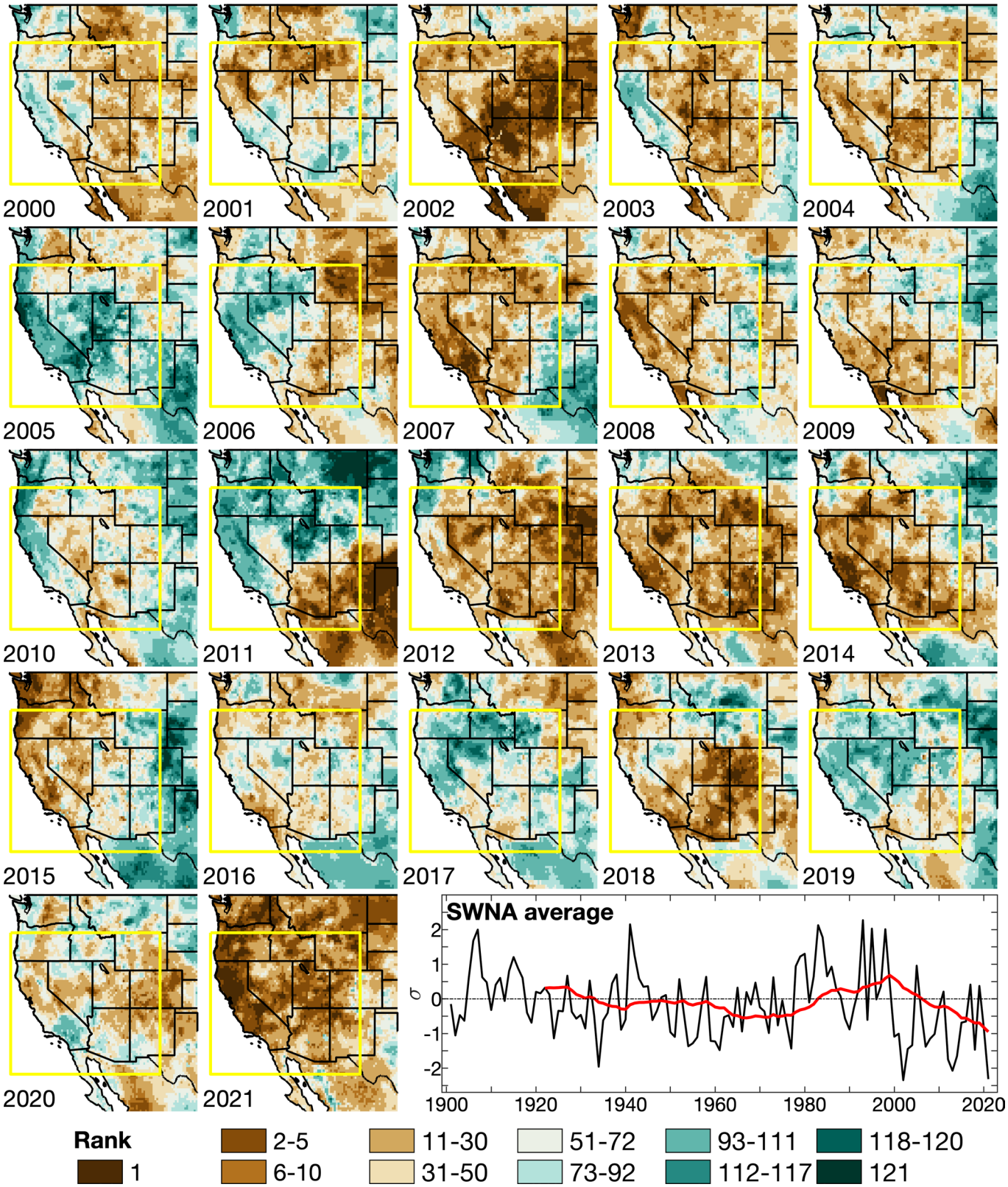

Extended Data Fig. 5 | Turn-of-the-21st-century drought in the western United States and northern Mexico. Ranking and time evolution of summer (June–August) drought severity as indicated by negative 0–200 cm soil moisture anomalies. Maps show how gridded summer drought severity in each year from 2000–2021 ranked among all years 1901–2021, where low (brown) means low soil moisture and therefore high drought severity. Yellow boxes bound the southwestern North America (SWNA) study region. Time series shows standardized anomalies (σ) of the SWNA regionally averaged soil moisture record relative to a 1950–1999 baseline. Black time series shows annual values and the red time series shows the 22-year running mean, with values displayed on the final year of each 22-year window. Geographic boundaries in maps were accessed through Matlab 2020a.

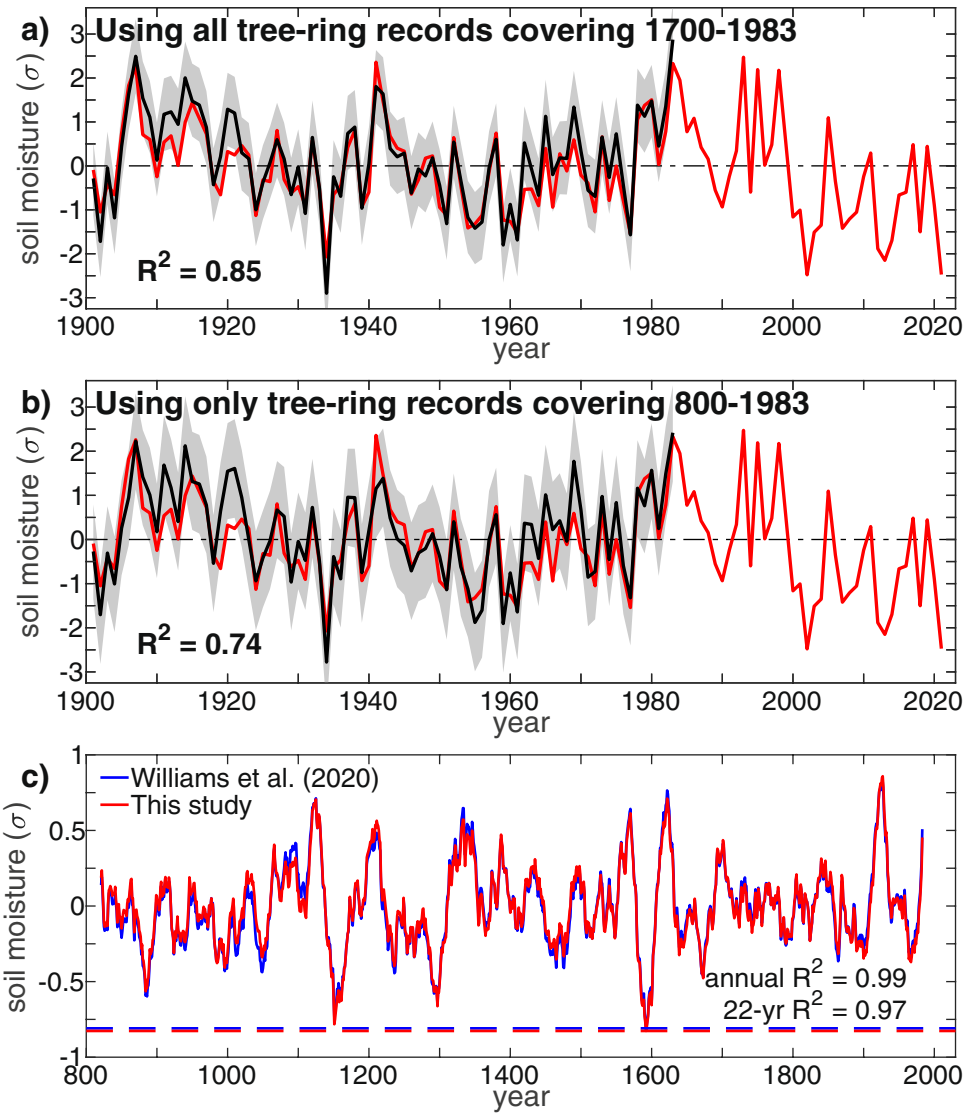

Extended Data Fig. 6 | Soil-moisture reconstruction skill. Cross-validated reconstruction skill using (**a**) all tree-ring chronologies that cover 1700–1983 and (**b**) only the subset of chronologies that cover 800–1983 to reconstruct southwestern North America (SWNA) regionally averaged summer soil moisture anomalies (black: cross-validated reconstruction, red: observed, grey shading: 95% confidence intervals). Cross-validated time series represent out-of-sample estimates made by repeatedly recalibrating the reconstruction algorithm while withholding a decade of data at a time from the calibration period (1901–1983) and making reconstruction estimates for each withheld decade (the final period withheld was longer than a decade: 1971–1983). In (**a** and **b**), soil moisture anomalies are standardized relative to 1921–2000. (**c**) Comparison of the 22-year running means of the SWNA regionally averaged soil moisture reconstructions produced for (red) this study versus (blue) Williams et al.[5]. In (**c**), records are standardized relative to (blue) 800–2021 and (red) 800–2018. Dashed red and blue horizontal lines represent each reconstruction's most negative 22-year mean anomaly, which in both reconstructions occurred in 1571–1592. R^2 values in **c** indicate the squared correlation between the two reconstructions during 800–1983 at the annual and 22-year running mean timescales.

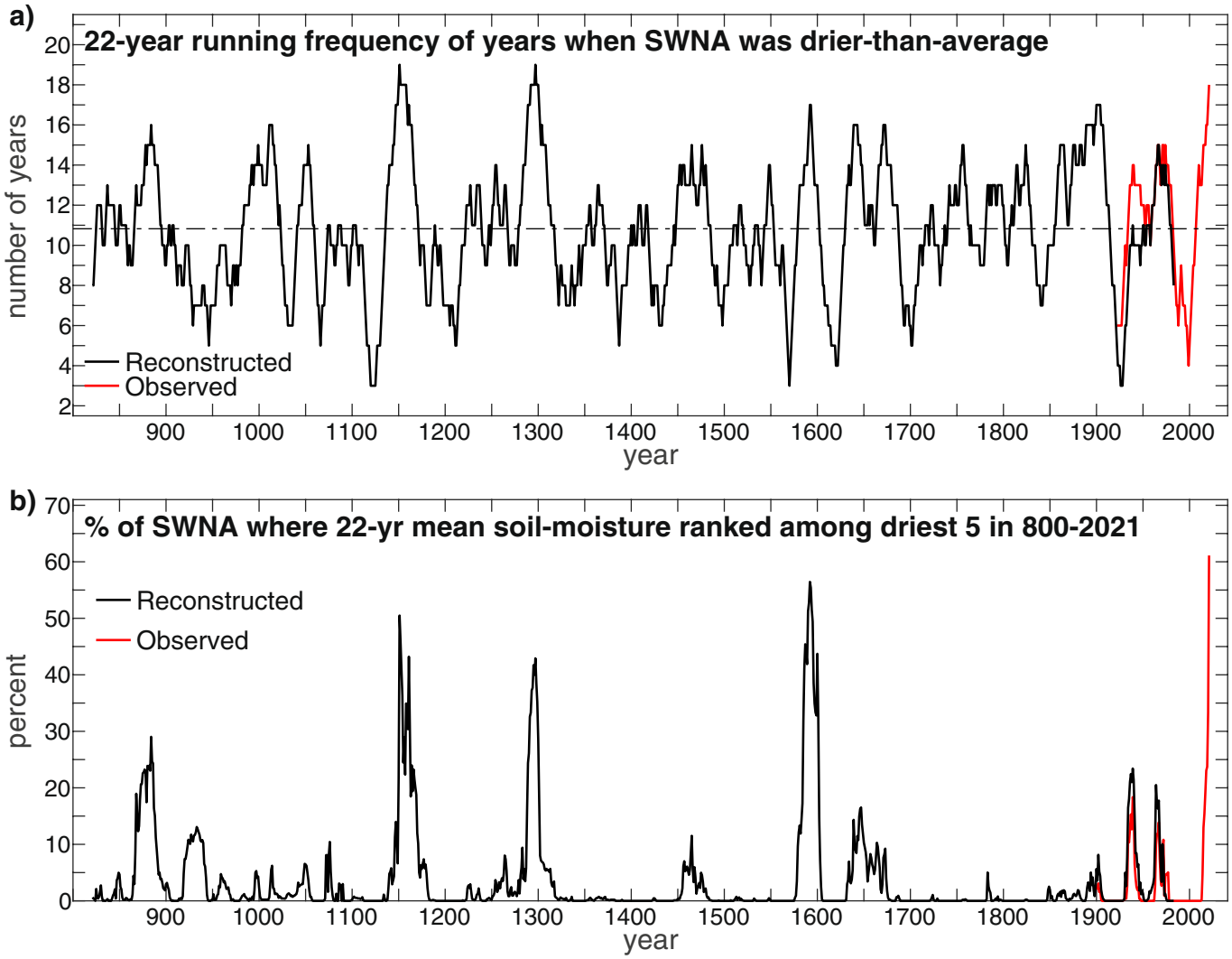

Extended Data Fig. 7 | Drought duration and extent. (**a**) Number of years in a running 22-year window when the 22-year mean summer soil moisture anomaly across southwestern North America (SWNA) was drier than the 800–2021 average. (**b**) The percentage of SWNA area where the 22-mean summer soil moisture was locally ranked in the top 5 driest 22-year periods in 800–2021.

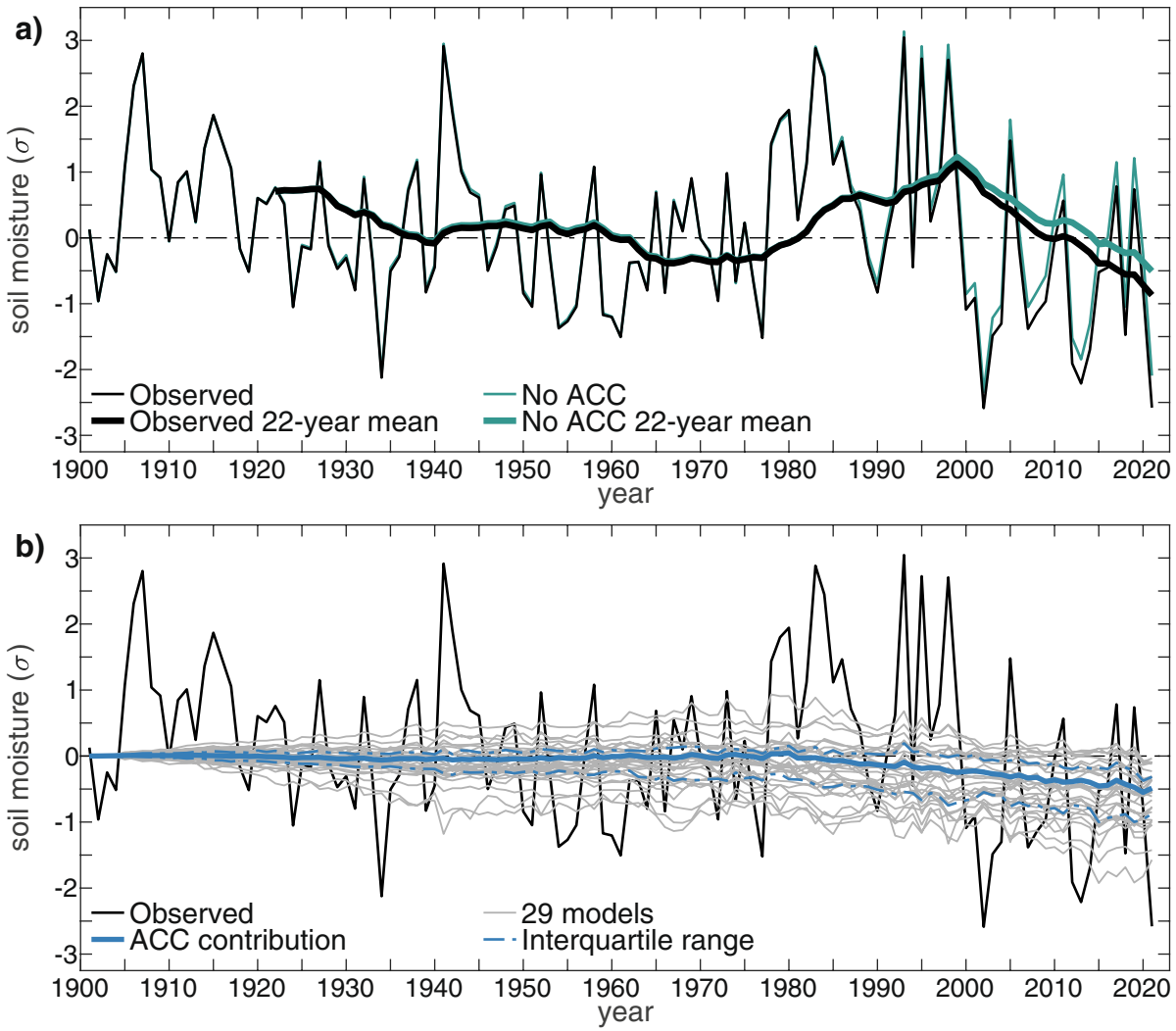

Extended Data Fig. 8 | Drought attribution. (**a**) Standardized anomalies (σ) of southwestern North American (SWNA) summer soil moisture calculated from (black) observed climate data and (turquoise) counterfactual climate data in which CMIP6 multimodel mean anthropogenic climate change (ACC) trends in temperature, relative humidity, and precipitation have been removed. (**b**) Same as (**a**) but the bold blue line shows the contribution of ACC, which is the bold black time series minus the bold turquoise time series in (**a**). Thin grey lines show results when the analysis is repeated removing climate trends simulated by each of the 29 CMIP6 individually (dotted blue lines show the interquartile values among the 29 grey time series). All standardization is relative to 800–2021, in which reconstructed values are used for 800–1900 and observation-based values are used for 1901–2021. Twenty-two year running means in (**a**) are displayed on the final year of each 22-year window.

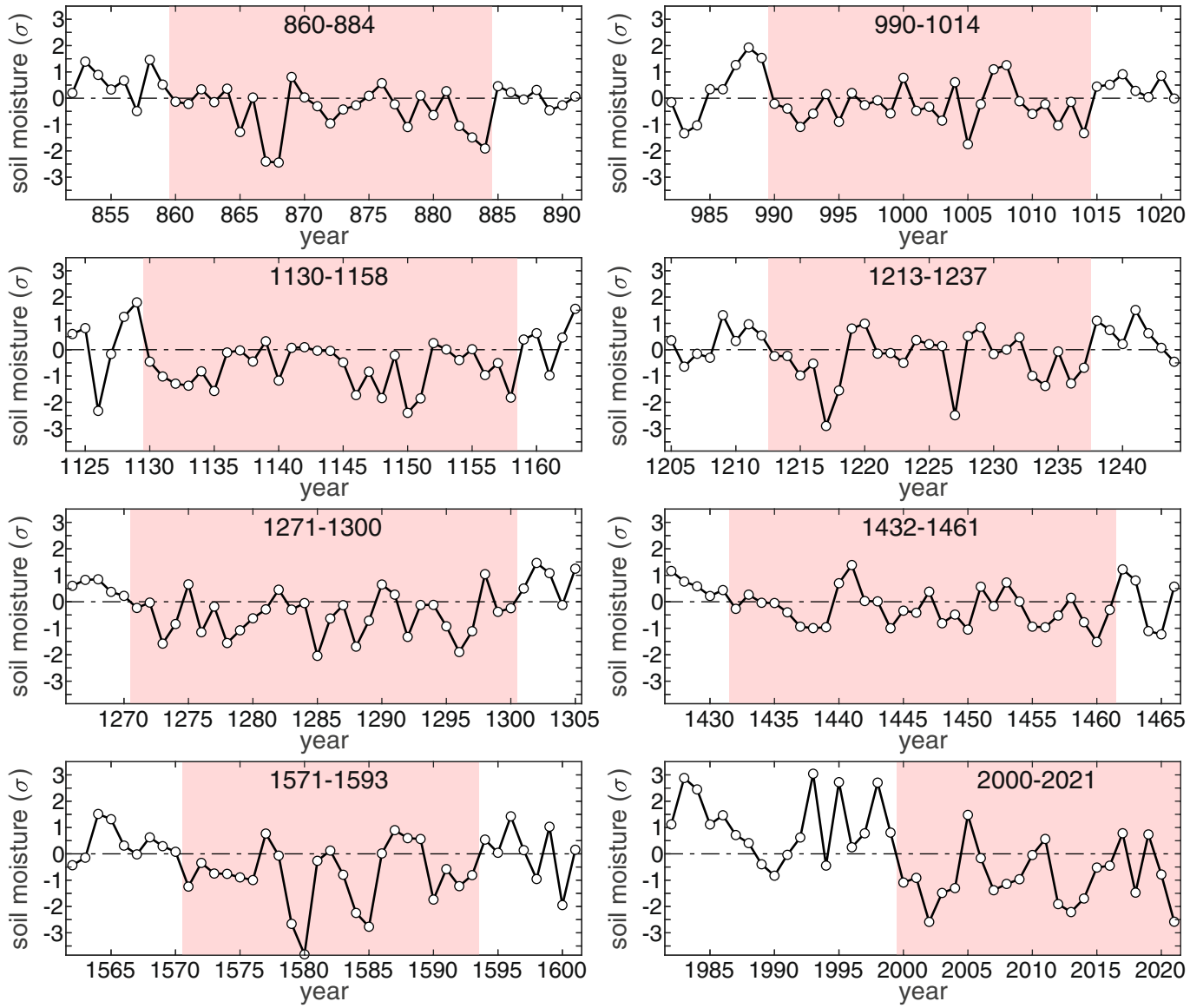

Extended Data Fig. 9 | Extended drought events. Summer soil moisture anomalies, expressed as standard deviations from the 800–2021 mean (σ), during the longest 8 extended drought events during the 800–2021 study period. The pink background bounds the years of each extended drought event. The horizontal dotted black line represents the 800–2021 mean. For the first 7 droughts shown, soil moisture anomalies come from our tree-ring reconstruction. For the final drought (2000–2021), anomalies come from our observation-based record.

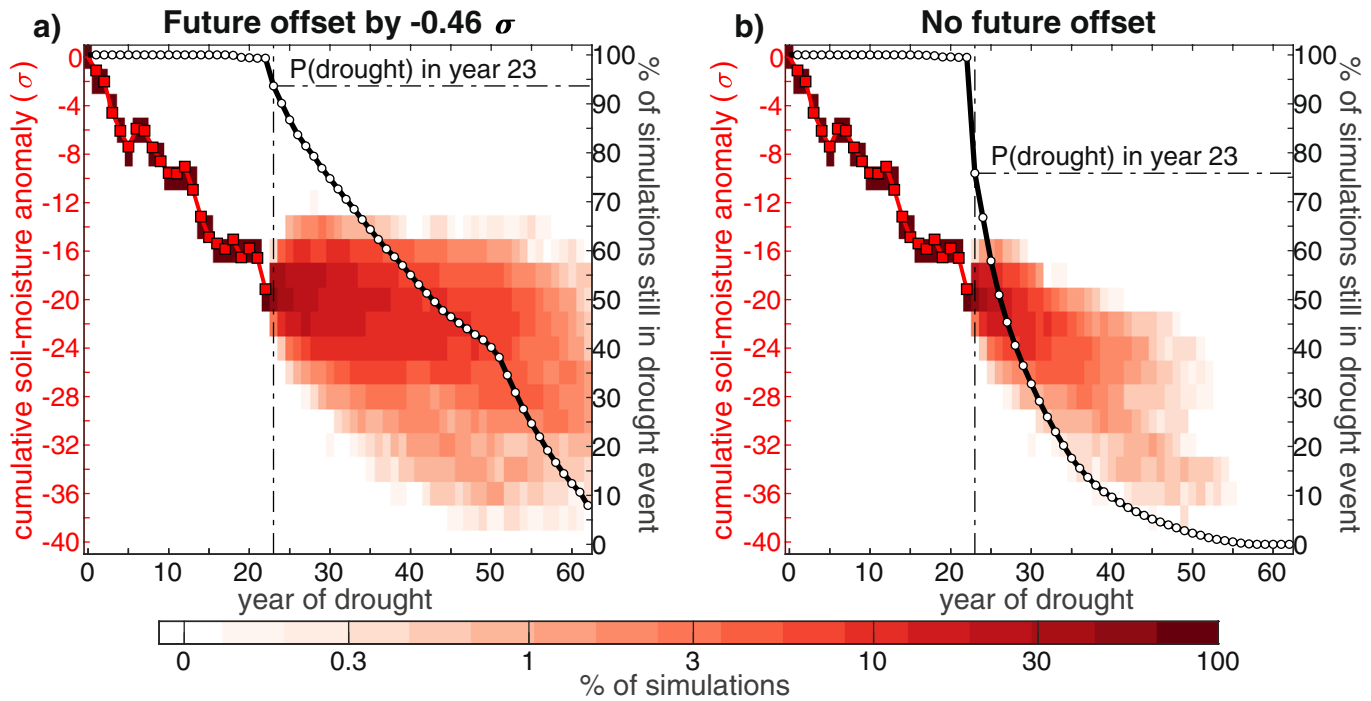

Extended Data Fig. 10 | Future drought trajectories. Simulated future trajectories of the turn-of-the-21st-century drought by extending the observed 2000–2021 record of southwestern North American soil moisture anomalies for 40 additional years (2022–2061) with each of the 1,183 40-year sequences from 800–2021. In both cases, when 2022–2061 soil moistures were replaced with 40-year soil moisture samples from within the observed period (1901–2021), we used soil moistures calculated after the removal of CMIP6 anthropogenic climate change (ACC) trends. In (a), 2022–2061 soil moisture anomalies were artificially dried by the 5-year mean ACC effect during 2017–2021 (−0.46 σ), representing a world in which the future drying effect from ACC is held at its 2017–2021 mean. In (b), no such adjustment to represent ACC drying is made, representing a future in which ACC has no effect. In both panels, the axis on the left corresponds to the red observed time series of cumulative soil moisture anomaly as well as the gridded percentages of the 1,183 simulations that result in a given cumulative soil moisture anomaly in a given year. The axis on the right corresponds to the black-and-white time series of the probability that the turn-of-the-21st-century drought survives to each year from 1 to 62. The vertical black dotted line identifies year 23, the duration of the shortest of the reconstructed megadroughts, and the horizontal black dotted line indicates the probability (P(drought)) that the turn-of-the-21st-century drought continues through a 23rd year. Determination of drought termination is made following the methods described in the Methods section.